Hindawi
Discrete Dynamics in Nature and Society
Volume 2023, Article ID 1465228, 11 pages
https://doi.org/10.1155/2023/1465228

*Research Article*

# A Mathematical Model on the Dynamics of In-Host Infection Cholera Disease with Vaccination

**Owade Kennedy Jackob, Okaka Akinyi, and Frankline Tireito**

*Department of Mathematics, Masinde Muliro University of Science and Technology, Kakamega, Kenya*

Correspondence should be addressed to Owade Kennedy Jackob; knowade@gmail.com

Received 20 December 2022; Revised 9 February 2023; Accepted 16 February 2023; Published 1 March 2023

Academic Editor: Filippo Cacace



In this paper, a within-host cholera mathematical model has been developed using a system of ordinary differential equations incorporating vaccine efficacy. The formulated model considers cells in an already vaccinated individual with a vaccine whose efficacy is $\gamma$. The solutions of the model have been shown to be both positive and bounded hence well-posed. The vaccine basic reproduction number has been carried out using the next generation matrix approach and is given by $R_{0V} = (\gamma/(d+\mu_2))$ and $R_{0V} < 1$ if $\gamma < (d+\mu_2)$. Analysis of the model shows that infection free equilibrium (IFE) point is both locally and globally asymptotically stable when $R_{0V} < 1$ and infection equilibrium (IE) point is locally asymptotically stable when $R_{0V} > 1$. Furthermore, analysis of the model shows that $R_{0V} < 1$ is not sufficient enough to eradicate in-host cholera disease, hence the existence of backward bifurcation which is an indication as to why cholera disease is persistent. To highlight the relevance of vaccine efficacy, a numerical simulation of the model with respect to vaccination is carried out and shows that when the vaccine efficacy $\gamma$ is high, there will be a lower infection rate of cells, hence the need to improve cholera vaccine efficacy.

## 1. Introduction

Cholera is an acute illness caused by an enterotoxin elaborated by *Vibrio cholerae* that when ingested colonises the small intestine. After 24 hrs to 48 hrs incubation period, cholera begins with sudden onset of painless water diarrhea that mainly quickly become voluminous and is often followed shortly by vomiting. In severe cases, stool volume can exceed 250 ml/kg in the first 24 hrs. Fever is usually absent, and muscle cramps due to electrolyte disturbances are common. The stool has a characteristic appearance; a nonbilious, grey, slightly cloudy fluid with flecks of mucus, no blood, and somewhat sweet and in-offensive odor. It has been called 'rice-water" stool because of its resemblance to the water in which rice has been washed. Clinical symptom parallel volume contraction shows losses of (3 – 5) percent of normal body weight. If fluids and electrolytes are not replaced, hypovolemic shock and death will occur [1].

According to the studies of natural infection, the human body has T-lymphocytes cell and B-lymphocytes cell which produce antibodies that attack the pathogen, thereby providing protection. However, in a situation of excess consumption of bacteria, the body may not defend itself; as a result, there is a need for vaccination [2].

The World Health Organization (WHO) recommends the use of oral cholera vaccines, Dukoral and Shanchol for those at high risk [3]. When these vaccines are administered, the cholera strain within the vaccine produces an incomplete, nontoxic version of the toxin; the body then responds to the safe version of cholera and creates immunity to the infection through the production of antibodies (T-lymphocytes cells and B-lymphocytes). Despite the availability and access to cholera vaccines, there is still a high burden of cholera in endemic areas [3].

Wang and Wang [4] developed a within-host dynamics of cholera with bacterial-viral interaction given as follows:

$$\frac{dB}{dt} = \Lambda - \alpha\frac{B}{K+B}V - \sigma_1 B,$$
$$\frac{dZ}{dt} = g(Z) + \theta_1\alpha\frac{B}{K+B}V - \sigma_2 Z, \quad (1)$$
$$\frac{dV}{dt} = h(V) + \theta_2\alpha\frac{B}{K+B}V - \sigma_3 V,$$

where $B$ represents environmental vibrios, $Z$ human vibrios, $V$ concentration of the virus, $\Lambda$ is the influx rate of the ingested environmental vibrios, $\alpha$ is the contact rate between the environmental vibrios and the virus, and $g(Z)$ and $h(V)$ intrinsic growth rate of $Z$ and $V$, respectively. Their main focus is the interaction of environmental vibrios, human vibrios, the virus, and the vibrios within the human host since such interaction is critical in shaping the evolution of the pathogen within the human body and directly contributes to the epidemiology of cholera at the population level since the human vibrios shed out of the human body will remain highly infectious for a certain period of time and can be transmitted among human hosts. They established the basic reproduction number as a sharp threshold for disease dynamics such that when $R_0 < 1$, the highly infectious vibrios will not grow within the human host, and the environmental vibrios ingested into the human body will not cause cholera infection and when $R_0 > 1$, the human vibrios will grow and persist, leading to human cholera.

Ratchford and Wang [5] developed a cholera within-host model for an average infected individual given as follows:

$$\frac{dZ}{dt} = C_1\mathrm{BV} - d_1\mathrm{MZ} - \epsilon Z,$$
$$\frac{dV}{dt} = C_2\mathrm{BV} - d_2\mathrm{MV} - \tau V, \quad (2)$$
$$\frac{dM}{dt} = e_1\mathrm{MZ} + e_2\mathrm{MV} - pM,$$

which is the fast scale system where $Z$, $V$, and $M$ represent the concentrations of human vibrios, pathogen, and host immune cells, respectively. The dynamics of the environmental evolution of the vibrios is governed by the equation given as follows:

$$\frac{dB}{dt} = \epsilon(Z)I - \delta B, \quad (3)$$

which is the low scale system, where $\epsilon Z$ is the host shedding rate that depends on the human vibrios. In their analysis, the within-host dynamical system proposed is expanded to include the influence of human virus and immune cell interaction with the infectious vibrios, and the findings show that the slow-scale and intermediate scale systems act predictably and the dynamics of two smaller combined systems depends mostly on $R_0$. However, the study recommends that a complete stability analysis of the equilibrium of the full system is of particular interest and it suggests that numerical simulation using real world data should be carried out to shed more light onto the likelihood of various assumptions. In this paper, the focus is to develop a within-host cholera model with vaccination investigating the impact of vaccination on the dynamics of in-host infection of cholera disease.

## 2. Model Formulation and Analysis

Cholera infection involves the interaction between the vibrio $V$ and the target cells $B$. The target cells $B$ are recruited at a constant rate $\Lambda$ and they die naturally at a rate $\mu_1$. Multiplication of the vibrio when infected cells are shed out is given by $\beta_V V$ within the human small intestine, where $h_V$ is the rate of recruitment of the vibrio. The interaction of vibrio within the small intestine with the target cells $B$ leads to the infection of target cells at the rate $\alpha BV$, where $\alpha$ is the contact rate between the target cells and the vibrios in the small intestine that leads to the production of infected cells $Z$. The infected cells die naturally at a rate $\mu_2$, and they are shed out at a rate $d$ due to the action of the vaccine. This shedding rate increases with an increase in vaccine efficacy. The saturation incidence rate is given by $(\alpha BV)/(1+\delta V)$ such that $\delta$ is the measure of saturation level of the vibrio. The natural clearance rate of the vibrio and shedding rate is given by $\sigma$ and $s$, respectively. The vaccine whose efficacy is $\gamma$ with the proportion of noneffectiveness of the vaccine given by $1-\gamma$ exposes an individual to a dose of live cholera bacteria, which causes the body to produce antibodies against the disease.The system of ordinary differential equation governing the description previously is as follows:

$$\frac{dB}{dt} = \Lambda - (1-\gamma)\frac{\alpha\mathrm{BV}}{1+\delta\mathrm{V}} - \mu_1 B + \gamma Z,$$
$$\frac{dZ}{dt} = -\gamma Z + (1-\gamma)\frac{\alpha\mathrm{BV}}{1+\delta\mathrm{V}} - (d+\mu_2)Z, \quad (4)$$
$$\frac{dV}{dt} = h_V + \beta_V V - (\sigma+s)V.$$

### 2.1. Assumptions of the Model

(i) There is the recovery of cells due to immunity gained as a result of vaccination

(ii) Target cells are recruited at a constant rate

## 3. Positivity and Boundedness of the Model

Since model [4] describes human cells, it should be well-posed. Thus, in this section, positivity and boundedness solutions are discussed. The positivity of solutions of the model [4] is determined using the following initial conditions [5]:

$$B(0) = B_0 \geq 0,$$
$$Z(0) = Z_0 \geq 0, \quad (5)$$
$$V(0) = V_0 \geq 0.$$

*3.1. Positivity of the Model*

**Proposition 1.** *Solutions of model (4) with the initial conditions (5) are positive in the region defined as* $\mathbb{R}_+ = \{(B, Z, V) | B \geq 0, Z \geq 0, V \geq 0\}$.

*Proof.* Let $N = \sup\{t > 0 | B \geq 0, Z > 0, V > 0\}$. The first equation of model (4) is given as follows:

$$\begin{aligned}\frac{\mathrm{d}B}{\mathrm{d}t} &= \Lambda - (1-\gamma)\frac{\alpha \mathrm{BV}}{1+\delta \mathrm{V}} - \mu_1 B + \gamma Z \\ &= \Lambda + \gamma Z - (1-\gamma)\frac{\alpha V}{1+\delta V} + \mu_1 \Big) B.\end{aligned} \tag{6}$$

From this, the integrating factor is $e^{\int_0^t (1-\gamma)(\alpha V(\tau)/1+\delta V(\tau))\mathrm{d}\tau + \mu_1(t)}$

Multiplying (6) by the integrating factor yields $dB(t)e^{(\int_0^t (1-\gamma)(\alpha V(\tau)/1+\delta V(\tau) d\tau + \mu_1(t))/\mathrm{d}t)} \geq (\Lambda + \gamma Z)e^{\int_0^t (1-\gamma)(\alpha V(\tau)/1+\delta V(\tau))\mathrm{d}\tau + \mu_1(t)}$

Solving the inequality yields $B(t)e^{\int_0^t (1-\gamma)((\alpha V(\tau))/1+\delta V(\tau))\mathrm{d}\tau + \mu_1(t)} - B(0) \geq \int_0^t (\Lambda + \gamma Z)e^{\int_0^k (1-\gamma)(\alpha V(\tau)/1+\delta V(\tau))\mathrm{d}\tau + \mu_1(k)\mathrm{d}k}$

Therefore, $B(t)$ becomes $B(t) \geq B(0)e^{-\int_0^t (1-\gamma)(\alpha V(\tau)/1+\delta V(\tau))\mathrm{d}\tau + \mu_1(t)} + e^{-\int_0^t (1-\gamma)\alpha V(\tau)/1+\delta V(\tau)\mathrm{d}\tau + \mu_1(t)} \times \int_0^t (\Lambda + \gamma Z)e^{\int_0^k (1-\gamma)(\alpha V(\tau)/1+\delta V(\tau))\mathrm{d}\tau + \mu_1(k)\mathrm{d}k} > 0$

Thus, $B(t) > 0$.

The second equation of the model (4) is given as follows:

$$\begin{aligned}\frac{\mathrm{d}Z}{\mathrm{d}t} &= -\gamma Z + (1-\gamma)\frac{\alpha \mathrm{BV}}{1+\delta \mathrm{V}} - (d+\mu_2)Z \\ &= (1-\gamma)\frac{\alpha \mathrm{BV}}{1+\delta \mathrm{V}} - (\gamma + d + \mu_2)Z.\end{aligned} \tag{7}$$

The integrating factor is $e^{\int_0^t (\gamma Z(\tau)\mathrm{d}\tau) + (\mathrm{d}+\mu_2)t}$

Multiplying (7) by the integrating factor yields $dZ(t)e^{\int_0^t (\gamma Z(\tau)\mathrm{d}\tau) + (\mathrm{d}+\mu_2)t}/\mathrm{d}t \geq (1-\gamma)(\alpha \mathrm{BV}/1+\delta \mathrm{V}) e^{\int_0^t (\gamma Z(\tau)\mathrm{d}\tau) + (\mathrm{d}+\mu_2)t}$

Solving the inequality yields $Z(t)e^{\int_0^t (\gamma Z(\tau)\mathrm{d}\tau) + (\mathrm{d}+\mu_2)t} - Z(0) \geq \int_0^t (1-\gamma)(\alpha \mathrm{BV}/1+\delta \mathrm{V})e^{\int_0^k (\gamma Z(\tau)\mathrm{d}\tau + (d+\mu_2)t)\mathrm{d}k}$

Therefore, $Z(t)$ becomes $Z(t) \geq Z(0)e^{-\int_0^t (\gamma Z(\tau)\mathrm{d}\tau)} + (\mathrm{d} + \mu_2)t + e^{-\int_0^t (\gamma Z(\tau)\mathrm{d}\tau) + (\mathrm{d}+\mu_2)t} \times \int_0^t (1-\gamma)(\alpha \mathrm{BV}/1+\delta \mathrm{V}) e^{\int_0^k (\gamma Z(\tau)\mathrm{d}\tau + (d+\mu_2)t)\mathrm{d}k} > 0$

Thus, $Z(t) > 0$.

In a similar manner to the third equation of the model (4) as follows:

$$\frac{\mathrm{d}V}{\mathrm{d}t} = h_V + \beta_V V - (\sigma + s)V. \tag{8}$$

From this, the integrating factor is $e^{\int_0^t (\sigma+s)\mathrm{d}t}$

Multiplying (8) by the integrating factor yields $(\mathrm{d}V(t)e^{\int_0^t (\sigma+s)dt}/\mathrm{d}t) \geq (h_V + \beta_V V)e^{\int_0^t (\sigma+s)\mathrm{d}t}$

Solving the inequality yields as follows:

$$V(t)e^{\int_0^t (\sigma+s)dt} - V(0) \geq \int_0^t (h_V + \beta_V V)e^{\int_0^k (\sigma+s)dk}. \tag{9}$$

Therefore, $V(t)$ becomes $V(t) \geq V(0)e^{-\int_0^t (\sigma+s)\mathrm{d}t} \times \int_0^t (h_V + \beta_V V)e^{\int_0^k (\sigma+s)\mathrm{d}k} > 0$.

Thus, $V(t) > 0$.

Hence, all the solution of model (4) given conditions (5) at any time $t$ are positive. Therefore, the population of target cells and infected cells in the human will continue to grow positively. □

*3.2. Boundedness of the Model.* Since the model formulated describes cells in a human being, the population of the target cells and the infected cells will always remain bounded.

**Proposition 2.** *Solutions of model (4) with the initial initial condtions (5) are bounded for* $\mathrm{t} \geq 0$ *in the region* $\Phi$ *given by* $\{\mathrm{B}(t)t + nZq(t)\} \in \mathbb{R}^3_+ : \mathrm{N} \leq (\Lambda/\mu)$.

*Proof.* Let $N(t) := B(t) + Z(t)$, where N is the total number of cells, and let $\mu = \mu_1 = \mu_2$. From the system of equation (4), we have

$$\begin{aligned} N'(t) &\leq \Lambda - (\mu_2 Z) \leq \Lambda - \mu N(t), \\ N'(t) &\leq \Lambda - \mu N(t), \\ \int N'(t)dt &\leq \int (\Lambda - \mu N(t))dt, \\ N(t)e^{\mu t} &\leq \int \frac{\Lambda}{\mu} e^{\mu t} dt, \\ N(t)e^{\mu t} &\leq \frac{\Lambda}{\mu} e^{\mu t} + C, \\ N(t) &\leq \frac{\Lambda}{\mu} + Ce^{-\mu t}, \\ \lim_{t \longrightarrow \infty} N(t) &\leq \frac{\Lambda}{\mu}. \end{aligned} \tag{10}$$

Hence, $N(t)$ is bounded, since solutions of model (4) are positive and bounded for $t \geq 0$; therefore, model (4) is mathematically and epidemiologically meaningful and is sufficient to consider its solution in $\Phi$. □

## 4. Basic Reproduction Number, $R_0$

The intervention strategy in this study is the vaccine efficacy; hence, the associated reproduction number is called vaccine reproduction number denoted as $R_{0V}$; it is the threshold

quantity that predicts the spread of cholera disease in a given population of the target cells in the presence of vaccination. Therefore, the vaccine reproduction number $R_{0V} = \rho(\mathrm{FK}^{-1})$ is the spectral radius of the matrix $\mathrm{FK}^{-1}$,
where

$$F = \begin{pmatrix} \gamma & -\dfrac{(1-\gamma)\alpha BV}{(1+\delta V)^2} \\ 0 & 0 \end{pmatrix}, \qquad K = \begin{pmatrix} d+\mu_2 & 0 \\ 0 & \beta-(\sigma+s) \end{pmatrix}, \tag{11}$$

Therefore,

$$R_{0V} = \mathrm{FK}^{-1} = \frac{\gamma}{(d+\mu_2)}. \tag{12}$$

The calculated $R_{0V}$ depends on vaccine efficacy and when $(d+\mu_2)$ is high due to the action of vaccine then $R_{0V} < 1$ which shows the elimination of infected cells due to the action of vaccine. The basic reproduction number, $R_{0V}$ being the measure of severity of an epidemic, determines whether or not cholera disease will invade the target cell population.

Epidemiologically, this implies that if $R_{0V} < 1$, cholera infection will die out in the cells and if $R_{0V} > 1$, cholera disease will persist in a cell population.

## 5. Stability Analysis

The stability at the IFE determines the short-term epidemics of the infection of cells, while its dynamics over a longer period of time is characterized by the global stability at the IFE. In this section, the analysis of local and global stability of IFE and local stability of IE is carried out.

*5.1. Existence of Infection-Free Equilibrium (IFE) Points.* These are steady state solutions in absence of cholera disease in the body; therefore, target cells are not infected. Stability analysis is carried out to predict the long-term behaviour of the solutions of the model (4).

**Proposition 3.** *For model (4), the* IFE *point is given by* $\mathrm{IFE} = (B^0, Z^0, V^0) = ((\Lambda/\mu_1), 0, 0)$.

*Proof.* At IFE, $Z = 0, V = 0$. Therefore, considering the first equation in the system (4) and replacing $Z = 0, V = 0$ and equating its right hand side to 0 yields

$$\Lambda - \mu_1 B = 0, \qquad \Lambda = \mu_1 B. \tag{13}$$

Making $B$ the subject yields

$$B = \frac{\Lambda}{\mu_1}. \tag{14}$$

Therefore, the infection-free equilibrium point of the system (4) is $((\Lambda/\mu_1), 0, 0)$. This shows that the infected class is zero since there are no pathogens and the entire population of cells consists of target cells only and their growth is bounded by $(\Lambda/\mu_1)$. □

*5.2. Local Asymptotic Stability of the Infection-Free Equilibrium (IFE)*

**Theorem 1.** *For any time $t \geq 0$, the infection-free equilibrium* $\mathrm{IFE} = ((\Lambda/\mu_1), 0, 0)$ *of model (4) is locally asymptotically stable when $R_{0V} < 1$ and unstable when $R_{0V} > 1$.*

*Proof.* The jacobian matrix of (4) is given as follows:

$$J = \begin{pmatrix} \dfrac{-(1-\gamma)\alpha V}{1+\delta V} - \mu_1 & \gamma & \dfrac{-(1-\gamma)\alpha\Lambda}{\mu_1(1+\delta V)^2} \\ \dfrac{(1-\gamma)\alpha V}{1+\delta V} & -\gamma-(d+\mu_2) & \dfrac{(1-\gamma)\alpha\Lambda}{\mu_1(1+\delta V)^2} \\ 0 & 0 & \beta_V-(\sigma+s) \end{pmatrix}. \tag{15}$$

The matrix (15) in terms of $R_{0V}$ yields

$$J_{IFE} = \begin{pmatrix} -\mu_1 & (d+\mu_2)R_{0V} & \dfrac{-(1-\gamma)\alpha\Lambda}{\mu_1} \\ 0 & -(d+\mu_2)(R_{0V}-1) & \dfrac{(1-\gamma)\alpha\Lambda}{\mu_1} \\ 0 & 0 & \beta_V-(\sigma+s) \end{pmatrix}. \tag{16}$$

To find the eigenvalues, we consider the characteristic equation $|J_{\mathrm{IFE}} - \lambda I| = 0$. For asymptotic stability, all the eigenvalues should be strictly negative. It can be seen clearly that $\lambda_1 = -\mu_1$ is one of the eigenvalues of (16).

Using Routh – Hurwitz Criterion for stability as used in [6] to determine the trace and determinant, let

$$\begin{vmatrix} -(d+\mu_2)(R_{0V}-1) & \dfrac{(1-\gamma)\alpha\Lambda}{\mu_1} \\ 0 & \beta_V-(\sigma+s) \end{vmatrix} = 0. \tag{17}$$

Equation (17) has

$$\mathrm{trace}(17) = -(d+\mu_2)(R_{0V}-1) + \beta_V - (\sigma+s) < 0, \tag{18}$$

and a $\mathrm{determinant}\det(17) = -(d+\mu_2)(R_{0V}-1)[\beta_V - (\sigma+s)] > 0$ iff $\beta_V < (\sigma+s)$. This implies that IFE is locally asymptotically stable when $R_0 < 1$ and unstable if $R_{0V} > 1$.

In Theorem 1, when cholera vaccine is administered, it implies that with a small perturbation of IFE, the solution of model (4) will eventually converge to IFE whenever $R_{0V} < 1$.

Epidemiologically, it implies that if a few infectious cholera pathogens are introduced into a population of target cells, the disease would die out when $R_{0V} < 1$; otherwise, the disease would spread into the population of target cells. □

*5.3. Global Stability of the Infection-Free Equilibrium (IFE).* The global stability of the IFE of model (4) is explored using Castilo–Chavez et al. [7]. Model (4) is rewritten in the form as follows:

$$\begin{aligned} \frac{dH}{dt} &= L(X, Z), \\ \frac{dZ}{dt} &= G(X, Z), \\ G(X, 0) &= 0, \end{aligned} \tag{19}$$

where $X \in \mathbb{R}^2$ denotes the uninfected compartments. At IFE,

$$\begin{aligned} \text{IFE} &= (X^*, Z^*), \\ X^* &= \left(\frac{\Lambda}{\mu_1}, 0\right). \end{aligned} \tag{20}$$

The conditions

$$\begin{aligned} \frac{dX}{dt} &= H(X, 0), X^*, \\ G(X, Z) &= \text{MZ} - \widehat{G}(X, Z), \widehat{G}(X, Z) \geq 0. \end{aligned} \tag{21}$$

$X^*$ is globally asymptotically stable,$6#where $M = D_Z G(X^*, 0)$ is a M-matrix (the off diagonal elements of $(M)$ and are non-negative). If model (4) satisfies the conditions previously (21), then Theorem 2 holds.

**Theorem 2.** *The fixed point* IFE $= (X^*, 0)$ *is globally asymptotically a stable equilibrium point of model (4) whenever the* $R_{0V} < 1$ *whenever the conditions (21) are satisfied, otherwise unstable.*

*Proof.* From model (4), we obtain

$$\begin{aligned} H(X, 0) &= \begin{pmatrix} \Lambda - \mu_1 B \\ 0 \\ 0 \end{pmatrix}, \\ G(X, Z) &= \text{MZ} - \widehat{G}(X, Z), \end{aligned} \tag{22}$$

where

$$\begin{aligned} M &= \begin{pmatrix} -(d + \mu_2)(R_{0V} - 1) & \dfrac{(1-\gamma)\alpha\Lambda}{\mu_1} \\ 0 & \beta_V - (\sigma + s) \end{pmatrix}, \\ \widehat{G}(X, 0) &= \begin{pmatrix} \widehat{G}_1(X, Z) \\ \widehat{G}_2(X, Z) \end{pmatrix} \\ &= \begin{pmatrix} 0 \\ 0 \end{pmatrix}. \end{aligned} \tag{23}$$

Since $\widehat{G}(X, Z) > 0$ and the conditions (21) are satisfied; therefore, IFE is globally asymptotically stable whenever $R_{0V} < 1$, otherwise unstable.

This implies that given a large perturbation of the IFE, the solutions of the model (4) will eventually converge to IFE whenever $R_{0V} < 1$. Epidemiologically, this means that if a large number of vibrios are introduced to a population of target cells, the disease would die off, hence the elimination of infection in cells since there are no secondary infection produced whenever $R_{0V} < 1$, otherwise the disease would persist. □

*5.4. Local Stability of the Infection Equilibrium (IE) Points.* Infection Equilibrium (IE) point is the state at which the disease persists in the cells. We investigate the local stability of infection equilibrium points at $E^*(B^*, Z^*, V^*)$.

**Theorem 3.** *The infection equilibrium point* $E^*(B^*, Z^*, V^*)$ *of system (4) is locally asymptotically stable whenever* $R_{0V} > 1$, *otherwise unstable.*

*Proof.* The infection equilibria $E^*(B^*, Z^*, V^*)$ of model (4) is obtained by equating model equations in (4) to zero then solving

$$\begin{aligned} \Lambda - (1 - \gamma)\frac{\alpha \text{BV}}{1 + \delta \text{V}} - \mu_1 B + \gamma Z &= 0, \\ -\gamma Z + (1 - \gamma)\frac{\alpha \text{BV}}{1 + \delta \text{V}} - (d + \mu_2) Z &= 0, \\ h_V + \beta_V V - (\sigma + s) V &= 0. \end{aligned} \tag{24}$$

The following equilibrium points are obtained by solving the previous equation simultaneously:

$$B^* = \frac{[(d+\mu_2)+\gamma][(1+\delta V^*)]Z^*}{(1-\gamma)\alpha V^*},$$
$$V^* = \frac{h_V}{(\delta+s)-\beta_V}. \tag{25}$$

Substituting $B^*$ into the second equation of model (4) and equating to zero, we obtain the following quadratic equation:

$$\gamma(d+\mu_2)Z^{*2} + \gamma(d+\mu_2)\alpha\frac{h_V}{\beta_V-(\delta+s)}Z^* + (d+\mu_2) = 0. \tag{26}$$

Let

$$\begin{aligned} a &= \gamma(d+\mu_2) = R_0(d+\mu_2)^2, \\ b &= \gamma(d+\mu_2)\alpha\frac{h_V}{\beta_V-(\sigma+s)} \\ &= R_0(d+\mu_2)^2\alpha\frac{h_V}{\beta_V-(\sigma+s)}, \\ c &= (d+\mu_2) = \frac{\gamma}{R_0}. \end{aligned} \tag{27}$$

The quadratic equation (26) can be written as follows (28):

$$\mathrm{aZ}^{*2} + \mathrm{bZ}^* + c = 0, \tag{28}$$

such that $Z^*$ is the positive solution of the equation (28). From preceding relations, $a$ is always positive.

Since $a > 0$, then there exist positive solutions of (28). Then, $aZ^{*2} + bZ^* + c = 0$ at $Z^* = 0 = c$ implying $c = 0$, then (28) has a unique endemic equilibrium point. Since $c = 0$, a unique solution of (28) is given by $Z^* = (-b/a)$, $b < 0$.

Consider the case when $R_{0V} < 1$ and $c > 0$. If $b \geq 0$, and using Descartes' rule of signs [8], $\mathrm{aZ}^{*2} + \mathrm{bZ}^* + c$ has no positive root.

If $b < 0$, then (28) is given as follows:

$$Z^* = \frac{b \pm \sqrt{b^2 - 4\mathrm{ac}}}{2a}. \tag{29}$$

Hence, the solutions are positive and distinct if $b^2 - 4\mathrm{ac} > 0$, in which case there are two endemic equilibria. The solutions of (28) coalesce into two roots when $b^2 - 4\mathrm{ac} = 0$ to form one endemic equilibrium point.

Now, if $b = \gamma(d+\mu_2)\alpha(h_V/\beta_V - (\sigma+s)) > 0$, $b$ will always be positive. To prove that infection equilibrium point $E^*$ is locally asymptotically stable when $R_{0V} > 1$, consider the Jacobian matrix of (4) evaluated at $E^*$ given as follows:

$$J_{E^*} = \begin{pmatrix} \frac{-(1-\gamma)\alpha V^*}{1+\delta V^*} - \mu_1 & \gamma & -\left[\frac{(1-\gamma)\alpha B^*}{(1+\delta V^*)^2}\right] \\ \frac{(1-\gamma)\alpha V^*}{1+\delta V^*} & -(d+\mu_2)(R_{0V}-1) & \left[\frac{(1-\gamma)\alpha B^*}{(1+\delta V^*)^2}\right] \\ 0 & 0 & \beta_V-(\sigma+s) \end{pmatrix}. \tag{30}$$

For the linearized system (4), the characteristic polynomial is expressed as follows:

$$|J - \lambda I| = 0. \tag{31}$$

When (30) is substituted into (31), it yields

$$\begin{bmatrix} \frac{-(1-\gamma)\alpha V^*}{1+\delta V^*} - \mu_1 - \lambda & (d+\mu_2)R_{0V} & -\left[\frac{(1-\gamma)\alpha B^*}{(1+\delta V^*)^2}\right] \\ \frac{(1-\gamma)\alpha V^*}{1+\delta V^*} & -(d+\mu_2)(R_{0V}-1) - \lambda & \left[\frac{(1-\gamma)\alpha B^*}{(1+\delta V^*)^2}\right] \\ 0 & 0 & \beta_V-(\sigma+s)-\lambda \end{bmatrix} = 0. \tag{32}$$

Solving (32) yields

$$\left[\frac{(1-\gamma)\alpha V^*}{1+\delta V^*} - \mu_1 - \lambda\right][(d+\mu_2)(R_{0V}-1)-\lambda][\beta_V-(\sigma+s)-\lambda] + \left[\left(\frac{(1-\gamma)\alpha V^*}{1+\delta V^*}\right][\beta_V-(\sigma+s)-\lambda][(d+\mu_2)(R_{0V}-1)] = 0. \tag{33}$$

Since $R_0 = (\gamma/d+\mu_2)$, then

$$\left[-\frac{(1-\gamma)}{1+\delta V^*}\alpha V^* - \mu_1 - \lambda\right][(d+\mu_2)(R_{0V}-1)-\lambda][\beta_V-(\delta+s)-\lambda] + (d+\mu_2)R_{0V}\left[\frac{(1-\gamma)}{1+\delta V^*}\alpha V^*\right][\beta_V-(\delta+s)-\lambda] = 0. \tag{34}$$

Let

$$\begin{aligned} m &= \left[\frac{(1-\gamma)}{1+\delta V^*}\alpha V^*\right], \\ n &= [\beta_V-(\sigma+s)], \\ V^* &= \frac{h_V}{\beta_V-(\delta+s)}. \end{aligned} \tag{35}$$

Then,

$$[m-\mu_1-\lambda]\left[(d+\mu_2)(R_{0V}-1)-\lambda\right][n-\lambda]+m(d+\mu_2)R_{0V}[n-\lambda]=0. \tag{36}$$

Expanding equation (36) yields

$$\left[\lambda^2+\lambda\left[(m-\mu_1)+(d+\mu_2)(R_{0V}-1)\right]+\left[(m-\mu_1)(d+\mu_2)(R_{0V}-1)\right)\right][n-\lambda]=0, \tag{37}$$

and gives

$$\begin{aligned} n-\lambda_1&=0,\\ \lambda_1&=n,\\ \lambda_1&=\beta_V-(\delta+s),\\ k&=\left[(m-\mu_1)+(d+\mu_2)(R_{0V}-1)\right],\\ \lambda_{2,3}&=\frac{-k\pm\sqrt{k^2-4(m-\mu_1)(d+\mu_2)(R_{0V}-1)}}{2}. \end{aligned} \tag{38}$$

Now, the eigenvalue $\lambda_1=[\beta_V-(\sigma+s)]$ has negative real parts, and the second eigenvalue is as follows:

$$\lambda_2=\frac{-k-\sqrt{k^2-4(m-\mu_1)(d+\mu_2)(R_{0V}-1)}}{2}, \tag{39}$$

and the third eigenvalue given is as follows:

$$\lambda_3=\frac{-k+\sqrt{k^2-4(m-\mu_1)(d+\mu_2)(R_{0V}-1)}}{2}. \tag{40}$$

If $4(m-\mu_1)(d+\mu_2)(R_{0V}-1) > [(m-\mu_1)+(d+\mu_2)(R_{0V}-1)]^2$, then the square root part of $\lambda_{2,3}$ yields an imaginary root; hence, a possibility of backward bifurcation [9] which is an indication of the oscillatory behaviour in cholera outbreaks; also, Theorem 3 implies that a small perturbation of IE, the solution of model [3], will always converge to IE whenever $R_{0V}>1$. Since $\lambda_1=\beta_V-(\delta+s)$ and $\lambda_{2,3}=(-k\pm\sqrt{k^2-4(m-\mu_1)(d+\mu_2)(R_{0V}-1)}/2)$ have negative real parts at infection equilibrium point, then infection equilibrium point is locally asymptotically stable whenever $R_{0V}>1$.

Epidemiologically implying that if vibrios are introduced in a population of target cells and there are new secondary infections produced whenever $R_{0V}>1$, then cholera disease would persist in the population of cells. The study of backward bifurcation in a disease dynamics can also occur when the reproduction number is less than unity, $R_{0V}<1$; this is explored in the next section. □

*5.5. Existence of Backward Bifurcation.* Based on the analysis in the previous section, there exists a range of values for $R_0$ in which model (4) have two positive endemic equilibria.

Let the discriminant $b^2-4ac$ be positive and be given as follows:

$$\left[\gamma(d+\mu_2)\alpha\frac{h_V}{\beta_V-(\sigma+s)}\right]^2-4\gamma(d+\mu_2)^2>0. \tag{41}$$

To find the value where the two endemic equilibria converge, set $b^2-4ac=0$ and solve for the value of $R_{0V}$ denoted $R_0^*$.

Let

$$b^2-4ac=0. \tag{42}$$

Then,

$$\begin{aligned} \frac{b^2}{4ac}&=1,\\ R_0^*&=1-\frac{b^2}{4ac},\\ b&=(1-\gamma)(d+\mu_2)\alpha\frac{h_V}{\beta_V-(\sigma+s)}. \end{aligned} \tag{43}$$

Let

$$\begin{aligned} R_0^*&=1-\frac{b^2}{4(1-\gamma)(d+\mu_2)^2}\\ &=1-\left[\frac{\alpha^2h_V^2(1-\gamma)}{\beta_V-(\sigma+s)}\right]. \end{aligned} \tag{44}$$

If $R_0^*<R_{0V}$ is equal to $b^2-4ac>0$, then backward bifurcation will occur for values of $R_{0V}$ such that $R_0^*<R_{0V}<1$. Therefore, we show the existence of backward bifurcation due to the existence of hyperbolic fixed points as in (39) and (40). Backward bifurcation in disease transmission models is where a stable endemic equilibrium coexists with a stable disease-free equilibrium when the associated reproduction number is less than unity.

Investigating the nature of bifurcation involving $IFE((\Lambda/\mu_1),0,0)$ using Castilo and Song [10], we consider a general system of ODEs given by (45):

$$\frac{dx}{dt}=f(x,\psi);\ f\colon R^n\times R^n,\ f\in C^2\left(R^n\times R^n\right). \tag{45}$$

**Theorem 4.** *Castilo–Chavez and Song [10]. We consider the following:*

(i) *Let* $I = D_x f(0,0)$ *be the linearization matrix of system (48) around the equilibrium point* $x = 0$ *with* $\psi$ *evaluated at 0. Zero is a simple eigenvalue of the matrix I and all other eigenvalues of I have negative real parts.*

(ii) *Matrix I has a non-negative right eigenvector w and a left eigenvector v corresponding to the zero eigenvalue*

(iii) *Let* $f_k$ *denote the* $k^{th}$ *component of* $f$ *and*

(a) $a_1 = \sum_{i,j,k=1}^{n} v_k w_i w_j (\partial^2 f_k / \partial x_i \partial x_j)(0,0)$

(b) $a_2 = \sum_{i,k=1}^{n} v_k w_i (\partial^2 f_k / \partial x_i \partial \phi)(0,0)$

*Then, the local dynamic of system (48) around* $x = 0$ *is determined by* $a_1$ *and* $a_2$.

(i) *If* $a_1 > 0$, $a_2 > 0$, *when* $\psi < 0$, *with* $|\psi| \ll 1$, *then* $x = 0$ *is locally asymptotically stable and there exists a positive unstable equilibrium and when* $0 < \psi \ll 1$, $x = 0$ *is unstable, and there exists a negative and locally asymptotically stable equilibrium.*

(ii) *If* $a_1 < 0$, $a_2 < 0$ *when* $\psi < 0$, *with* $|\psi| \ll 1$, *then* $x = 0$ *is unstable; when* $0 < \psi \ll 1$, $x = 0$ *is locally asymptotically stable and there exists a positive unstable equilibrium.*

(iii) *If* $a_1 > 0$ *and* $a_2 < 0$ *when* $\psi < 0$, *with* $|\psi| \ll 1$, *then* $x = 0$ *is unstable, and there exists a locally asymptotically stable negative equilibrium, when* $0 < \psi \ll 1$, $x = 0$ *is stable and positive unstable equilibrium appears.*

(iv) *When* $a_1 < 0$ *and* $a_2 > 0$, *then there exists a forward bifurcation.*

(v) *When* $a_1 > 0$ *and* $a_2 > 0$, *then the bifurcation at* $\psi = 0$ *is backward.*

*Proof.* Using Castillo–Chavez and Song [10], let $\psi$ be the bifurcation parameter such that $R_{0V} < 1$ such that $x_0$ is an IFE equilibrium for all values of $\psi$.

We consider

$$\frac{dx}{dt} = f(x, \psi), \tag{46}$$

where $f$ is a continuous differentiable function at least twice in both $x$ and $\psi$. The IFE is the line $(x_0, \psi)$ and local stability of the IFE changes at the point $(x_0, \psi)$.

Let

$$\begin{aligned} B &= x_1, \\ Z &= x_2, \\ V &= x_3. \end{aligned} \tag{47}$$

System (4) becomes

$$\begin{aligned} \frac{dx_1(t)}{dt} &= \Lambda - (1-\gamma)\frac{\alpha x_1(t) x_3(t)}{1 + \delta x_3(t)} - \mu_1 x_1(t) + \gamma x_2(t) =: f_1, \\ \frac{dx_2(t)}{dt} &= -\gamma x_2(t) + (1-\gamma)\frac{\alpha x_1(t) x_3(t)}{1 + \delta x_3(t)} - (d + \mu_2) x_2(t) =: f_2, \\ \frac{dx_3(t)}{dt} &= h_V + \beta_V V - (\sigma + s) x_3(t) =: f_3. \end{aligned} \tag{48}$$

Applying Theorem 4 to investigate if system (48) exhibits a backward bifurcation when $R_{0V} = 1$. Therefore, we first linearize the system and then compute its eigenvalues and eigenvectors corresponding to eigenvalues with negative real part form a basis for the stable eigenspace.

Linearizing (48) around the IFE yields

$$\begin{pmatrix} -\mu_1 & (d + \mu_2) R_{0V} & \dfrac{-(1-\gamma)\alpha\Lambda}{\mu_1} \\ 0 & -(d + \mu_2)(R_{0V} - 1) & \dfrac{(1-\gamma)\alpha\Lambda}{\mu_1} \\ 0 & 0 & \beta_V - (\sigma + s) \end{pmatrix}. \tag{49}$$

The eigenvalues of (49) are given by $\lambda_1 = -\mu_1, \lambda_2 = -(d + \mu_2)(R_{0V} - 1)$, and $\lambda_3 = \beta_V - (\sigma + s)$.

Now, let $w = (w_1, w_2, w_3)^T$ be the right eigenvector associated with zero eigenvalue. Hence,

$$\begin{pmatrix} -\mu_1 & (d + \mu_2) R_{0V} & \dfrac{-(1-\gamma)\alpha\Lambda}{\mu_1} \\ 0 & -(d + \mu_2)(R_{0V} - 1) & \dfrac{(1-\gamma)\alpha\Lambda}{\mu_1} \\ 0 & 0 & \beta_V - (\sigma + s) \end{pmatrix} \begin{pmatrix} w_1 \\ w_2 \\ w_3 \end{pmatrix} = 0. \tag{50}$$

which yields

$$\begin{aligned} -\mu_1 w_1 + (d + \mu_2) R_{0V} w_2 - \frac{(1-\gamma)\alpha\Lambda}{\mu_1} w_3 &= 0, \\ -\left[(d + \mu_2)(R_{0V} - 1)\right] w_2 + \frac{(1-\gamma)\alpha\Lambda}{\mu_1} w_3 &= 0, \\ \left[\beta_V - (\sigma + s)\right] w_3 &= 0. \end{aligned} \tag{51}$$

Solving for $w_1$, $w_2$, and $w_3$, we obtain $w_1 = 2(1-\gamma)\alpha\Lambda$, $w_2 = (1-\gamma)\alpha\Lambda/\mu_1(d + \mu_2)(R_{0V} - 1)$, and $w_3 = 1$.

Let $v = (v_1, v_2, v_3)^T$ be the left eigenvector associated with zero eigenvalue such that

$$\begin{pmatrix} -\mu_1 & 0 & 0 \\ (d+\mu_2)R_{0V} & -(d+\mu_2)(R_{0V}-1) & 0 \\ \dfrac{-(1-\gamma)\alpha\Lambda}{\mu_1} & \dfrac{(1-\gamma)\alpha\Lambda}{\mu_1} & \beta_V-(\sigma+s) \end{pmatrix} \begin{pmatrix} v_1 \\ v_2 \\ v_3 \end{pmatrix} = 0,$$

$$-\mu_1 v_1 = 0,$$

$$[(d+\mu_2)R_{0V}]v_1 - [(d+\mu_2)(R_{0V}-1)]v_2 = 0,$$

$$\left[\frac{-(1-\gamma)\alpha\Lambda}{\mu_1}\right]v_1 + \left[\frac{(1-\gamma)\alpha\Lambda}{\mu_1}\right]v_2 + [\beta_V-(\sigma+s)]v_3 = 0. \tag{52}$$

Solving for $v_1$, $v_2$, and $v_3$, we obtain $v_1 = 0$, $v_2 = 0$, and $v_3 = 1$.

It is observed that $v.w = 1$. Now, evaluating the partial derivatives of system (48) at IFE, we obtain

$$\frac{\partial^2 f_1}{\partial x_1 \partial x_3} = \frac{\partial^2 f_1}{\partial x_3 \partial x_1} = \frac{-(1-\gamma)\alpha}{\delta},$$
$$\frac{\partial^2 f_2}{\partial x_1 \partial x_3} = \frac{(1-\gamma)\alpha}{\delta}. \tag{53}$$

Since all the other remaining second order partial derivatives are equal to zero. Thus, computing the coefficients $a_1$ and $a_2$ is defined in Theorem 4 (iii).

$$a_1 = \sum_{i,j,k=1}^{n} v_k w_i w_j \frac{\partial^2 f_k}{\partial x_i \partial x_j},$$
$$a_2 = \sum_{i,k=1}^{n} v_k w_i \frac{\partial^2 f_k}{\partial x_i \partial x_j}. \tag{54}$$

We consider system (48) and considering $a_1$ and $a_2$ only as the nonzero derivatives for the terms $(\partial^2 f_k/\partial x_i \partial x_j)$ and $(\partial^2 f_k/\partial x_i \partial x_j)$, it follows that

$$a_1 = 2v_3 w_1 w_3 \frac{\partial^2 f_2}{\partial x_1 \partial x_3} + v_3 w_2 w_1 \frac{\partial^2 f_1}{\partial x_3 \partial x_1},$$
$$a_2 = v_3 w_1 \frac{\partial^2 f_2}{\partial x_1 \partial x_3} + v_3 w_2 \frac{\partial^2 f_2}{\partial x_1 \partial x_3} + v_3 w_3 \frac{\partial^2 f_2}{\partial x_1 \partial x_3}. \tag{55}$$

Substituting $v_s$ and $w_s$ in (55) yields

$$a_1 = 2\frac{(1-\gamma)^2\alpha^2\Lambda}{\delta},$$
$$a_2 = \frac{(1-\gamma)\alpha}{\delta}\left[1 + \frac{(1-\gamma)\alpha\Lambda}{\mu_1(d+\mu_2)(R_{0V}-1)} + 2(1-\gamma)\alpha\Lambda\right]. \tag{56}$$

The signs of coefficients $a_1$ and $a_2$ determine the nature of bifurcation exhibited by system (4) around the infection-free equilibrium for $R_{0V} = 1$.

Table 1: Parameter values for the within-host cholera model.

| Description | Parameters | Initial value | Source |
|---|---|---|---|
| Recruitment rate of B | $\Lambda$ | $1.0 * 10^6$ cells | [11] |
| Natural death rate of B | $\mu_1$ | 0.27 day$^{-1}$ | [5] |
| Natural death rate of Z | $\mu_2$ | 0.27 day$^{-1}$ | [5] |
| Contact rate of B and V | $\alpha$ | 0.9 | [5] |
| Clearance rate of V | $\sigma$ | 0.02 | [5] |
| Vaccine efficacy | $\gamma$ | 0.66 | [3] |
| Recruitment rate of V | $h_V$ | 0.7 | [11] |
| Shedding rate of V | $s$ | 0.03 | [11] |
| Multiplication rate of V | $\beta_V$ | 0.3 | [11] |

For model (4) to undergo backward bifurcation, then $a_1 > 0$ and $a_2 > 0$. We consider the parameter values used in Table 1 to verify the conditions $a_1 > 0$ and $a_2 > 0$ where

$$a_1 = 2\frac{(1-\gamma)^2\alpha^2\Lambda}{\delta},$$
$$a_2 = \frac{(1-\gamma)\alpha}{\delta}\left[1 + \frac{(1-\gamma)\alpha\Lambda}{\mu_1(d+\mu_2)(R_{0V}-1)} + 2(1-\gamma)\alpha\Lambda\right]. \tag{57}$$

Let $\alpha = 0.9$, $0 < \gamma < 1$, $\delta = 0.05$, $d = 0.4$, and $\mu_1 = \mu_2 = 0.27$ substituting these numerical values in $a_1$ and $a_2$ yields $a_1 > 0 = 3.24 * 10^3$ and $a_2 > 0 = 2.68304 * 10^5$. Hence, model (4) exhibits backward bifurcation. This implies that the epidemiological implication in relation to cholera disease of backward bifurcation is that $R_{0V} < 1$ is necessary and not sufficient for effective control of cholera disease; hence in a backward bifurcation setting, the cholera disease will invade to a relatively high endemic level in cells. □

## 6. Numerical Simulation

In this section, we give some numerical simulation to illustrate our theoretical results by numerically solving the model system (4). This is carried out by first taking the initial values from the existing literature as shown in Table 1. Using the parameter values in Table 1 and fitting the model system (4) in MATLAB software, the ode45 command in MATLAB is used to solve it and the results in Section 6.2 are obtained.

*6.1. Parameter Values.* The parameters values are described in Table 1.

*6.2. Simulation Results.* The graphs and the results obtained are described as in Figures 1–4.

Figure 1–3 shows a graph of target cells $B$, infected cells $Z$, and the vibrio $V$ against time in hours when $\gamma = 0.1$, when $\gamma = 0.6$ and when $\gamma = 0.9$, respectively.

In Figure 1, it is observed that if the vaccine efficacy is low i.e., $\gamma = 0.1$, there are more cells infected which is an indication that there are pathogens invading the target cells in the small intestine as a result decrease in number of target cells as they become infected due to their interaction with the pathogen. This implies that the lower the vaccine efficacy, the higher the rate of infection of target cells.

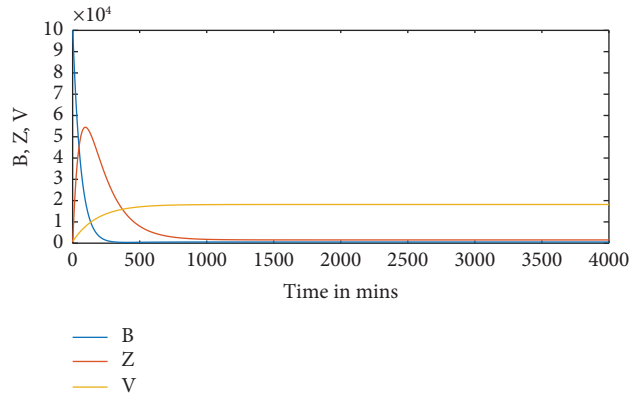


Figure 1: Graph of $(B, Z, V)$ against time when $\gamma = 0.1$.

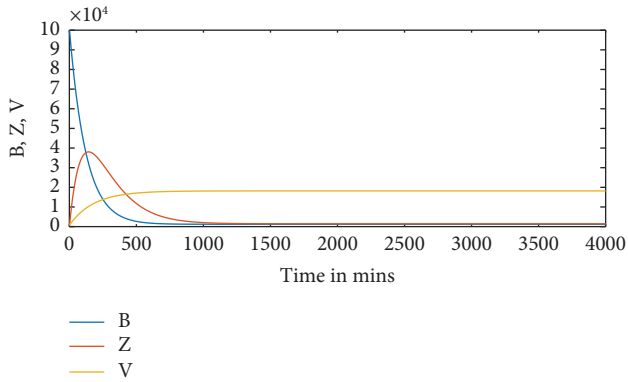


Figure 2: Graph of $(B, Z, V)$ against time when $\gamma = 0.6$.

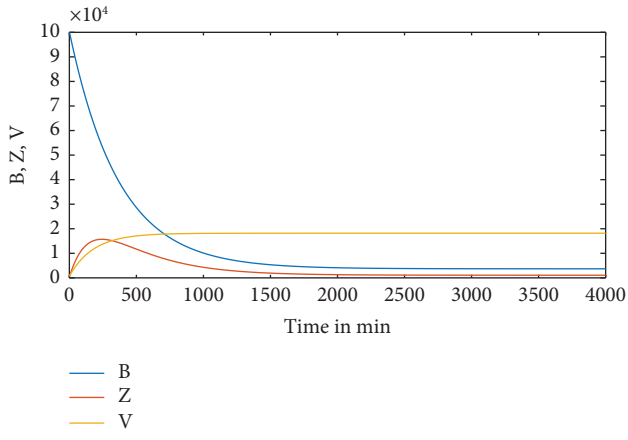


Figure 3: Graph of $(B, Z, V)$ against time when $\gamma = 0.9$.

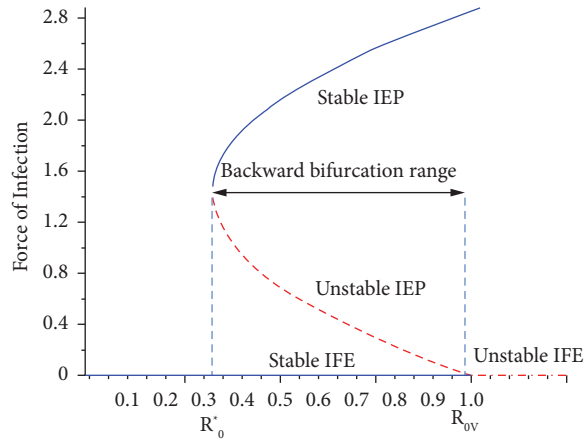


Figure 4: Bifurcation curve.

In Figure 2, the vaccine efficacy is $\gamma = 0.6$, the number of cells infected decreases compared to when $\gamma = 0.1$. This shows that with improved vaccine efficacy, there will be low infection of cells without which the vibrios will continue to invade the cells to cause infection and this explains why cholera disease is persistence.

In Figure 3, the vaccine efficacy is $\gamma = 0.9$; this leads to decrease in the number of cells infected which implies that with vaccine efficacy being high, the chances of cells getting infected will be low compared to when the vaccine efficacy is low. It also implies that when the vaccine efficacy is high, it takes longer time for healthy cells to be infected. Despite this, vibrios still find their way to infect the cells.

Figure 4 shows backward bifurcation diagram for the force of infection against reproduction number of model (4) using parameter values $\alpha = 0.9$, $\gamma = 0.66$, $\delta = 0.05$, $d = 0.4$, and $\mu_1 =$

$\mu_2 = 0.27$. This shows that backward bifurcation occurs for values of $R_{0V}$ such that $R_0^* < R_{0V} < 1$, hence reoccurrence of in-host infection cholera disease when $R_{0V} < 1$.

## 7. Conclusion

In this paper, a within-host cholera model with vaccination is developed and analysed. The existence and stability of the steady states of model have been determined and show that it is locally and globally asymptotically stable when $R_{0V} < 1$ and unstable when $R_{0V} > 1$. The analysis of the model also shows that infection equilibrium point is locally asymptotically stable when $R_{0V} > 1$; this means that there is persistent infection. Furthermore, analysis shows that when the vaccine efficacy $\gamma$ is high, there is high clearance rate of $Z$ and $V$. In this study, $R_{0V} < 1$ is not sufficient enough to eradicate in-host cholera disease; as a result, model (4) undergoes backward bifurcation indicating coexistence of infection-free equilibrium point and infection equilibrium point when $R_{0V} < 1$ and this explains why cholera disease has remained persistently endemic. Since in the model analysis, it is observed that when vaccine efficacy is high, the number of cells getting infected reduces. The study, therefore, recommends that vaccines with high efficacy than the currently existing vaccines should be manufactured. This could help reduce the burden of cholera disease when there is an outbreak.

## Data Availability

The data used to support the findings of the study are included in the article.

## Conflicts of Interest

The authors declare that they have no conflicts of interest.

## Acknowledgments

The authors would like to thank their supervisors Dr. Colleta Akinyi and Dr. Frankline Tireito.

## References

[1] B. Fauci, Isselbacher, H. Kasper, and H. Wilson, "Pinciples of internal medicine," *Journal of Biological Dynamics*, vol. 2, no. 7, pp. 020291–020295, 1998.

[2] World Health Organization, "Cholera vaccines," *WHO position paper*, vol. 85, no. 13, pp. 117–128, 2010.

[3] World Health Organization, "Cholera vaccines," *WHO position paper*, vol. 92, no. 34, pp. 477–500, 2017.

[4] X. Wang and J. Wang, "Modeling the within-host dynamics of cholera: bacterial-viral interaction," *Journal of Biological Dynamics*, vol. 11, no. 2, pp. 484–501, 2017.

[5] C. Ratchford and J. Wang, "Modeling cholera dynamics at multiple scales: environmental evolution, between-host transmission, and within-host interaction," *Mathematical Biosciences and Engineering*, vol. 16, no. 2, pp. 782–812, 2019.

[6] K. F. Tireito, G. O. Lawi, and C. O. Okaka, "HIV/AIDS treatment model with the incorporation of diffusion equations," *Applied Mathematical Sciences*, vol. 12, no. 12, pp. 603–615, 2018.

[7] C. Castillo-Chavez, Z. Feng, and W. Huang, "On the computation of $R_0$ and its role on global stability," in *Mathematical Approaches for Emerging and Reemerging Infectious Diseases*, vol. 125 no. 3, p. 229550, Springer, NewYork, NY, USA, 2002.

[8] X. Wang, "A simple proof of descartes's rule of signs," *The American Mathematical Monthly*, vol. 111, no. 6, p. 525, 2004.

[9] J. Arino, C. C. Mc Cluskey, and P. Van Den Driessche, "Global results for an epidemic model with vaccination that exhibits backward bifurcation," *SIAM Journal on Applied Mathematics*, vol. 64, no. 1, pp. 260–276, 2003.

[10] C. Castillo-Chavez and B. J. Song, "Dynamical models of tuberculosis and their applications," *Mathematical Biosciences and Engineering*, vol. 1, no. 2, pp. 361–404, 2004.

[11] D. Schugar, *Virus-Cell Interaction and Viral Antimetabolies*, Shugar Academic Press, New York, NY, USA, 1972.